BIOCHEMISTRY
including biophysical chemistry & molecular biology

Article

pubs.acs.org/biochemistry

Anionic Lipid Binding to the Foreign Protein MGS Provides a Tight Coupling between Phospholipid Synthesis and Protein Overexpression in *Escherichia coli*

Candan Ariöz,* Weihua Ye, Amin Bakali, Changrong Ge, Jobst Liebau, Hansjörg Götzke, Andreas Barth, Åke Wieslander, and Lena Mäler*

Center for Biomembrane Research, Department of Biochemistry and Biophysics, Stockholm University, SE-106 91 Stockholm, Sweden

Supporting Information

ABSTRACT: Certain membrane proteins involved in lipid synthesis can induce formation of new intracellular membranes in *Escherichia coli*, i.e., intracellular vesicles. Among those, the foreign monotopic glycosyltransferase MGS from *Acholeplasma laidlawii* triggers such massive lipid synthesis when overexpressed. To examine the mechanism behind the increased lipid synthesis, we investigated the lipid binding properties of MGS *in vivo* together with the correlation between lipid synthesis and MGS overexpression levels. A good correlation between produced lipid quantities and overexpressed MGS protein was observed when standard LB medium was supplemented with four different lipid precursors that have significant roles in the lipid biosynthesis pathway. Interestingly, this correlation was highest concerning anionic lipid production and at the same time dependent on the selective binding of anionic lipid molecules by MGS. A selective interaction with anionic lipids was also observed *in vitro* by ^{31}P NMR binding studies using bicelles prepared with *E. coli* lipids. The results clearly demonstrate that the discriminative withdrawal of anionic lipids, especially phosphatidylglycerol, from the membrane through MGS binding triggers an *in vivo* signal for cells to create a "feed-forward" stimulation of lipid synthesis in *E. coli*. By this mechanism, cells can produce more membrane surface in order to accommodate excessively produced MGS molecules, which results in an interdependent cycle of lipid and MGS protein synthesis.

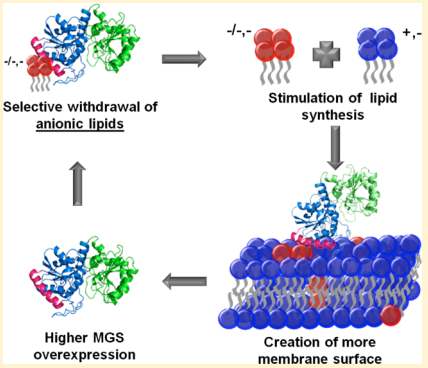

The importance of the plasma membrane (PM) in living cells originates from its unique features, which define a regulatory selective barrier between the cytoplasm and the outer environment. This regulatory barrier controls a directed flux of vital molecules in and out of the cytoplasm, maintaining the homeostasis of the cell.[1] The constituents of the PM are mainly phospholipids and membrane proteins, and the correct environment to fold properly for the latter is provided by phospholipids.[2] Most bacterial species lack internal membranes, but some are observed to have internal membrane systems in addition to the plasma membrane.[3] Naturally occurring proteins in a few bacteria can induce organelle-like internal membrane systems, which are derived from the cytoplasmic membrane. Moreover, overexpression of certain natural and foreign membrane proteins in *Escherichia coli* (*E. coli*) also seems to trigger formation of new plasma membrane extensions, folded to either vesicles, tubes, or flat "sacks" in the cytoplasm.[4−11] The actual mechanism behind the creation of artificially induced internal membrane systems is not yet clear, but the increased transmembrane protein quantities may induce membrane curvature stress by their "wedge-like" packing shapes or simply by crowding on the membrane surface with different oligomerization states.[12]

Another possibility for triggering a vesiculation event is provided by the membrane-interface anchoring of monotopic proteins through electrostatic and hydrophobic interactions with phospholipid headgroups.[4−6] Common features of these vesicle inducing proteins include their localization at the interface of a single bilayer leaflet, enrichment in positively charged amino acids at the positions in contact with the membrane interface, and their ability to induce membrane expansions through increased lipid production in the cell.[13]

The monotopic lipid glycosyltransferase monoglucosyldiacylglycerol synthase (MGS) from *Acholeplasma laidlawii* (*A. laidlawii*) has been shown to be expressed to a very high yield in *E. coli*.[14] Concomitantly, large quantities of membranous vesicles were detected to be formed intracellularly. Two other glycosyltransferases, the endogenous *E. coli* MurG and LpxB involved in peptidoglycan and lipopolysaccharide syntheses, respectively, were also reported to stimulate lipid synthesis when overexpressed from similar expression vectors.[5,6] These two proteins are structurally very similar to MGS, i.e.,

Received: May 16, 2013
Revised: July 19, 2013
Published: July 19, 2013

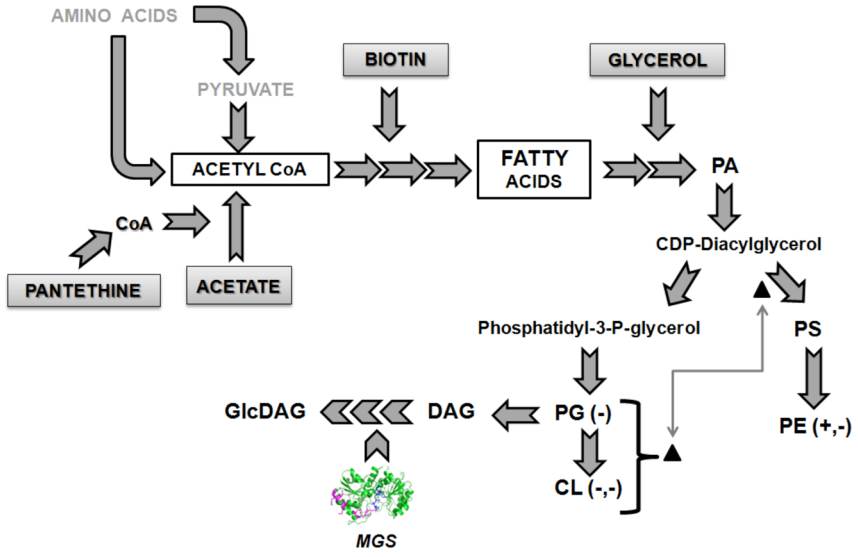

Figure 1. Biosynthetic pathway for membrane lipid synthesis in *E. coli* cells. In normal LB broth, lipids are known to be synthesized from growth medium-derived amino acids (upper left corner-shaded in gray). Supplementation with acetate, glycerol, pantethine, and biotin (gray colored boxes) affects lipid synthesis. The full arrows indicate the metabolic steps in *E. coli*, and the broken arrow symbolizes the additional step including the "foreign" GlcDAG synthesis (from PG-derived DAG) by MGS glycosyltransferase. ↔ indicates the regulatory relationship between anionic PG and CL species and PssA, which is known to be dependent on the surface charge properties of inner membranes.

monotopic proteins with two Rossmann fold domains.[15,16] The degree of vesiculation observed for MGS was, however, higher than for the two other glycosyltransferases.

MGS synthesizes the lipid α-glucosyldiacylglycerol (GlcDAG) from UDP-Glc and DAG,[16] but inactive mutants of the protein have been shown to equally well induce vesicle formation in *E. coli*.[13] The increased membrane production by overexpression of MGS presumably occurs because of a need for more lateral membrane areas for MGS insertion, but what could be the potential factor, or factors, triggering phospholipid stimulation in the cells? To address this question, we have in this study investigated the factors governing the increased lipid production by MGS in *E. coli*. We have examined the effects of selectively adding key lipid precursors (such as acetate) on the lipid synthesis and MGS expression.

The total quantity and composition of membrane phospholipids in *E. coli* are rarely varied by extrinsic or intrinsic factors, unless a triggering signal changes the production rate of the *E. coli* lipid synthesis pathway (Figure 1). The distribution between the major species of the membrane phospholipids thus remains constant, with 75% of zwitterionic phosphatidylethanolamine (PE), 20% of anionic phosphatidylglycerol (PG), and 5% of cardiolipin (CL).[2] The rate of PG synthesis can be increased manyfold without changes in membrane lipid molar fractions,[17] strongly supporting a basic control mechanism dependent on the bilayer properties, such as charge density, as demonstrated for a key enzyme responsible for PE synthesis.[18]

From previous work, an increased anionic lipid content, i.e. PG and CL, in bilayers *in vitro* is known to strongly promote MGS binding to membranes and thus enhance its enzymatic activity.[19,20] However, no experimental data indicating anionic lipid binding to MGS *in vivo* have been obtained so far. Therefore, we have used a combination of chromatographic and spectroscopic techniques to investigate in detail the lipid-binding properties of MGS. We report that a preferential binding of the overexpressed monotopic MGS to anionic lipids triggers a response promoting the total lipid production in the cell, which in turn results in an interactive cycle between phospholipid synthesis and protein production.

EXPERIMENTAL PROCEDURES

Growth and Overexpression Conditions. The MGS gene from *Acholeplasma laidlawii* was previously cloned into a pET-15b vector (Novagen), containing an N-terminal 6xHis tag, which was introduced in an *E. coli* strain BL21-AI (Invitrogen). Transformants (BL21 AI-MGS) were selected with 100 μg/mL carbenicillin. Protein overexpression in the BL21 AI-MGS strains was started by preparation of an overnight culture prepared in either 2xLuria−Bertani Broth (2xLB, 20 g/L Tryptone (Fluka), 10 g/L Bacto-yeast extract (Fluka), 10 g/L NaCl (Sigma)), and/or Terrific Broth (1xTB, 12 g/L Tryptone (Fluka), 24 g/L Bacto-yeast extract (Fluka), 4 mL/L glycerol, 2.3 g/L KH_2PO_4, 12.5 g/L K_2HPO_4) media supplemented with appropriate antibiotics. The inoculation was 2% (v/v) from overnight cultures to the freshly prepared 2xLB (or 1xTB if indicated) medium, followed by growth at 37 °C with 200 rpm shaking until OD_{600} values of ∼0.3−0.4 were reached. At this point the temperature was lowered to 22 °C, and gene expression was induced with 0.2% (w/v) L-arabinose and 1 mM isopropyl-β-D-1-thiogalactopyranoside (IPTG). After 22 h of induction, cells were harvested by centrifugation at 5600 rpm (∼3200 × *g*) at 4 °C for 20 min and were further washed with 100 mM 4-(2 hydroxyethyl)-1-piperazineethanesulfonic acid (HEPES) buffer (pH 8), flash frozen, and kept at −80 °C until used.

Lipid Analysis Using a Mild Detergent Solubilization. To study the binding of detergent-purified MGS and two inactive mutants, E300A and E308A[13] to *E. coli* lipids, cells were grown in 50 mL of 1xTB medium containing 20 μCi/mL of [1-^{14}C] acetate (55.3 mCi/mmol) (GE Healthcare), and cell pellets were obtained as described previously.[13] Pellets (MGS and the two mutant proteins) were lysed for 60 min at 4 °C with 25 mL lysis buffer (50 mM HEPES, pH 8, 1 mg/mL lysozyme, 0.1 mg/mL DNase, and 1 complete protease inhibitor cocktail tablet (EDTA-free) (Roche Applied Science)

dx.doi.org/10.1021/bi400616n | *Biochemistry* 2013, 52, 5533−5544

per 50 mL of liquid) per gram of wet cell pellet. The collected membranes were then solubilized at 4 °C for 2 h with 100 mL of solubilization buffer (50 mM HEPES, pH 8, 20 mM $MgCl_2$, 1.16 M glycerol, 500 mM NaCl, 2 mM DDM, 1 complete protease inhibitor cocktail (EDTA-free), and 1 mM TCEP) per gram of cells. A clearified supernatant was obtained by centrifugation at 4500 rpm for 60 min at 4 °C, prior to Ni-NTA resin purification, and the supernatant was incubated overnight with 4 mL of Ni-NTA agarose resin (QIAGEN) containing 20 mM imidazole. Resins were washed extensively with 50 column volumes of washing buffer (50 mM HEPES, pH 8, 20 mM $MgCl_2$, 1.16 M glycerol, 500 mM NaCl, 0.1 mM DDM, 1 mM TCEP, and 20 mM imidazole) and transferred to a lipid-free glass tube in order to analyze lipids from MGS and reduce the detergent amounts. Lipids were extracted from purified proteins using a standard Bligh & Dyer extraction protocol,[21] and detergent removal was performed by extensive washing of the chloroform phases with ∼300 mL of double-distilled water, which withdraws DDM monomers to the water phase due to its monomeric water solubility. The amount of lipids was determined using thin layer chromatography (TLC). Concentrated extracts (obtained by drying under N_2) were all applied on standard silica gel 60 TLC plates (Merck) and developed in a chloroform/methanol/acetic acid 85:25:10 (v/v) solvent system in one dimension. TLC plates were incubated (after drying) with a PhosphoImager (FujiFilm) screen for 20 h. Lipids were visualized and quantified by calibrated electronic autoradiography. The imager response was calibrated by spotting eight series of [1-^{14}C]acetic acid samples on the dried TLC plate before exposure, ranging between 25−500 nCi and 25−3750 nCi, respectively. The count responses were completely linear for these series, with $R^2 \geq 0.99$ for both.

Detergent-Free Protein Purification. Pellets from 1L LB culture were lysed by sonification in 140 mL of lysis buffer (50 mM sodium phosphate buffer (pH 7.5) supplemented with 0.3 mg/mL DNase, 1 mg/mL lysozyme). The cell lysate was centrifuged for 30 min at 10 000 × *g*, and the resulting supernatant was subjected to ultracentrifugation (40 000 rpm using a Ti 45 rotor for 1 h) to collect vesicle membranes. The vesicle membranes were homogenized in 70 mL of 100 mM Na_2CO_3 (pH 11) in order to extract MGS. The homogenate was subjected to a second ultracentrifugation step, and the supernatant that contains the soluble form of MGS was purified on 4 mL of Q-Sepharose FF resin (GE Healthcare). The resin was washed thoroughly with wash buffer (10 mM Na_2CO_3, 10% glycerol, 1 mM β-mercaptoethanol), and the bound MGS was eluted by a step gradient (10 mM Na_2CO_3 pH 11, 10% glycerol, 1 mM β-mercaptoethanol, and 0.5 M NaCl). The eluted protein could typically be concentrated to above 10 mg/mL (Amicon ultra 10K MWCO, Millipore), and the buffer was exchanged with a mini dialysis unit (Slide-A-lyser 10K MWCO, Pierce). Labeled lipids copurified with MGS were extracted, separated, and analyzed as described above.

Bicelle Preparation. Two bicelle systems[22−26] made up of lipids isolated from the membranes of BL21 AI-MGS *E. coli* cells grown in 2xLB were prepared. 1,2-Dihexanoyl-*sn*-glycero-3-phosphocholine (DHPC, Avanti Polar Lipids, Alabaster, AL) was used as the detergent. Membrane associated divalent ions were removed after chloroform:methanol (2:1; v/v) extraction by washing the lipid extracts with NMR buffer (20 mM PIPES, 1 mM EDTA, 150 mM NaCl, 0.002% NaN_3, and 10% D_2O at pH 7.4). The chloroform phases were further purified with adsorption chromatography using a silica gel column. *E. coli* phospholipids from the membranes were collected from the methanol fraction after the removal of DAG/fatty acids with chloroform and GlcDAG lipids with acetone washes. Phospholipid and GlcDAG fractions were pooled and concentrated to 60 and 75 mg/mL, respectively. The purity was very high, and lipid stocks were kept at −20 °C until used.

The total concentration of lipids + DHPC was 75 or 150 mM, and the molar ratio of lipid to detergent (*q*-value) was maintained at 0.5 in all samples. One bicelle system was made to mimic a normal *E. coli* lipid composition[2] (−GlcDAG bicelles: with 65% PE, 30% PG, and 5% CL) and another to mimic the conditions where MGS was overexpressed (+GlcDAG bicelles: 50% PE, 20% PG, 5% CL, and 25% GlcDAG). The bicelles were prepared by drying purified *E. coli* lipids under a stream of nitrogen gas, and the produced lipid films were then dispersed in a solution of DHPC and NMR buffer by extensive vortexing. The samples were transferred to NMR tubes and subjected to six cycles of freeze−thawing.

NMR Spectroscopy. ^{31}P NMR spectra were recorded on a Bruker Avance spectrometer operating at 14.1 T (243 MHz ^{31}P frequency), equipped with a 5 mm TXI probe. All NMR measurements were conducted at 25 °C. ^{31}P 90° pulse lengths were between 22 and 24 μs. All ^{31}P NMR experiments were recorded with a 1 kHz sweep width using 2400 data points and ^{1}H gated decoupling. The spectra were processed with 0.5 Hz line broadening and referenced externally to phosphoric acid. To study the influence of MGS on the lipids, spectra with increasing concentrations of MGS, ranging from 0 to 0.2 mM, were recorded. Longitudinal relaxation times (T_1) were measured for bicelles without MGS and with 0.14 mM MGS using an inversion recovery pulse sequence with ^{1}H decoupling throughout the experiment using the following relaxation delays: 0.001, 0.01, 0.1, 0.2, 0.35, 0.55, 0.75, 1, 1.2, 1.5, 2, 3, 5, and 9 s. Transverse relaxation times (T_2) were measured using the CPMG pulse sequence with ^{1}H decoupling during acquisition using the following total CPMG delays: 2, 10, 20, 30, 50, 80, 120, 160, 200, and 250 ms. The errors in T_1 and T_2 values were estimated from three individual measurements.

^{31}P pulsed field gradient diffusion experiments were recorded to ascertain the morphology of the q = 0.5 bicelles with GlcDAG. In this way, diffusion coefficients for all phospholipids could be determined separately. Translational diffusion coefficients were determined using the Stejskal−Tanner spin-echo pulse sequence with a fixed diffusion time and a pulsed field gradient increasing linearly over 16 steps.[27,28] The gradient was calibrated using the ^{1}H signal of a standard sample containing 1% H_2O in D_2O, 0.1 mg/mL $GdCl_3$, and 0.1% DSS. The experiments were repeated twice using two individual samples.

Experimental Design for Stimulation of Lipid Synthesis. To examine the potential coupling between lipid synthesis and MGS synthesis, BL21 AI-MGS cells were grown in 10 mL of 2xLB medium supplemented with different combinations of acetate, glycerol, biotin, and pantethine in various concentration ranges (see Table S2). All supplements were prepared freshly and filtered/autoclaved just before addition to the growth media. Cells were grown and induced, and cell pellets were collected as described previously. For protein analysis, cell pellets were solubilized with 10 freeze−thaw cycles in a solubilization buffer containing 50 mM HEPES, 300 mM NaCl, 10 mM $MgCl_2$, 1.16 M glycerol, 0.5 mM tris(2-carboxyethyl)phosphine hydrochloride (TCEP), 0.1 mg/mL DNAase, and 15 mM CHAPS detergent (Sol grade,

dx.doi.org/10.1021/bi400616n | *Biochemistry* 2013, 52, 5533−5544

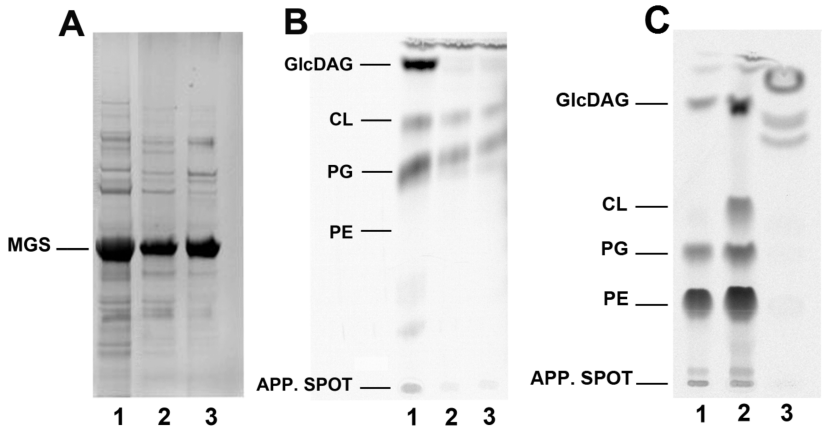

Figure 2. Strong interaction of MGS with anionic lipids *in situ*. (A) Stained SDS-PAGE gel with purified (1) MGS (wild type), (2) E300A inactive MGS mutant, and (3) E308A inactive MGS mutant. (B) TLC analysis of radioactive endogenous lipids labeled with ^{14}C-acetate during overexpression of (1) MGS, (2) E300A, and (3) E308A proteins extracted using the "mild" solubilization protocol. (C) Analysis of radioactive endogenous lipids copurified with MGS extracted by the detergent-free protocol. In (C), lane 1 shows total lipid extracts from uninduced BL21 AI-MGS cells, lane 2 induced BL21 AI-MGS cells, and lane 3 TLC analysis of purified MGS-by Na_2CO_3 extraction. No phospholipids were observed to be copurified with MGS during Na_2CO_3 extraction. All samples were treated identically, and lipid standards were run on the same plate in order to observe TLC migration profiles.

Affymetrix). SDS-PAGE and Western blots were performed with the clearified supernatants, and proteins were detected with Penta-His antibody (BSA-free, QIAGEN) and Goat antimouse IgG HRP conjugate. The blots were visualized with ECLPlus Western Blotting Detection kit (GE-Healthcare), recorded with a CCD camera, and quantified with ImageGauge 4.0 software (FujiFilm Science Lab).

For lipid analysis, cells were grown as for the protein analysis and the lipids were extracted from collected cell pellets according to the same procedure given above. Lipids in chloroform phases were then concentrated, applied on a TLC plate, and developed as described earlier. TLC plates were dried, stained with iodine (vapor) for visualization, and recorded with a CCD camera. All lipid bands were calibrated by application of 100 μg of CL lipid on each plate and quantified by ImageGauge version 4.0. Lipids from similar OD_{600} absorbance units were applied on the TLC plates except for the high glycerol + high acetate combination, a condition that retards the cell growth. All lipid extracts obtained from these cell pellets were applied on the TLC plates, and responses were normalized by dividing the imager responses by the relevant OD_{600} values.

Multivariate Data Analysis. Multivariate data analysis (MVDA) was used to analyze the effect of stimulation of lipid synthesis on the MGS expression. The four precursors and cofactors used in the experimental setup—acetate, glycerol, biotin, and pantethine—were selected as input variables. The amounts of these precursors/cofactors were defined as three levels (high-H, medium-M, and low-L values), and they were chosen based on single-component experiments. A 2^4 full factorial design with 16 experimental points was chosen to investigate all possible corners of the four-dimensional hypercube including 2 replicated center points, representing possible combinations of the amounts of precursors/cofactors. The amounts of the four major synthesized lipids (PE, PG, CL, and the "foreign" GlcDAG) present in the bacterial membranes, detected by the TLC assay, together with the amount of overexpressed MGS, detected by Western blotting, were defined as responses after normalization with relevant OD_{600} values. The software MODDE 9.0 (Umetrics AB, Sweden) was used for creating the experimental design, constructing, evaluating, and interpreting the model by partial least-squares analysis (PLS).

Fourier Transform Infrared Spectroscopy. Phospholipid and protein amounts, as well as acetate incorporation into the fatty acid tails, were monitored using Fourier transform infrared (FT-IR) spectroscopy. BL21 AI (without MGS) and BL21 AI-MGS (with MGS) cells were grown in 2xLB medium (as described previously) supplemented either with 300 mM undeuterated (C^1H_3COONa) or with deuterated sodium acetate (C^2H_3COONa, 99%; Cambridge Isotope Laboratories). To analyze similar cell amounts for each sample, the absorbance at 600 nm ($OD_{600\ nm}$) was measured prior to centrifugation, and culture volumes were adjusted in each sample. Then cells were harvested by centrifugation (5600 rpm/20 min/4 °C) and resuspended in FT-IR buffer (100 mM HEPES and 20 mM $MgCl_2$). Since we found that BL21 AI-MGS cells produced considerably more membranes and proteins compared to BL21 AI cells, the samples originating from BL21 AI-MGS cells had to be diluted more than BL21 AI cells to keep the maximum absorbance in the infrared spectral range close to 1.0, where the accuracy of the measurement is high. 10 μL of these diluted samples were applied directly on a CaF_2 IR-window and dried under gentle N_2 gas flow. Spectra were recorded in transmission mode with freshly collected (intact) cells using a Bruker VERTEX 70 spectrometer equipped with a HgCdTe detector. Spectra of the extracted lipids from the corresponding samples were recorded in the same way. All measurements were repeated at least five times with preparations from independent cell cultures. The spectra were analyzed with the OPUS spectrometer software (Bruker Optics), using bands near ~1654 cm^{-1} corresponding to amide I vibrations from proteins and ~1740 cm^{-1} corresponding to υ(C═O) vibrations from lipids. To estimate the amount of incorporated deuterium in the lipids, lipid CD stretching bands were integrated between 2037 and 2264 cm^{-1} and compared to the CH stretching bands, integrated between 2754 and 3048 cm^{-1}. The bands originate only from the lipids, as remaining acetate will not be present in the chloroform extracts of the lipids. The bands were integrated separately for each sample

dx.doi.org/10.1021/bi400616n | *Biochemistry* 2013, 52, 5533−5544

with respect to a baseline drawn between the integration limits. The standard deviations for all these measurements were less than 0.1 (σ = 0.068) with a linear regression coefficient of R^2 = 0.99. The CD band areas were normalized using a correction factor (1.54) obtained from spectra of a 1:1 mixture of deuterated and undeuterated acetate since the absorption of CD vibrations is weaker than that of CH vibrations.[29]

Promoter Activity Assay. The presence of a possible genetic regulation[30] involved in the increased lipid synthesis was studied using a promoter activity assay where GFP fused regions (plasmids) to the promoters of rpoE, PlsB, cfa, and psD from the *E. coli* Promoter Collection (Thermo Scientific) were introduced into *E. coli* BL21 AI and BL21 AI-MGS (MGS producing) cells separately. Transformants were selected on LB agar supplemented with 25 μg/mL kanamycin for BL21 AI variants and 25 μg/mL kanamycin + 100 μg/mL carbenicillin for BL21 AI-MGS variants. Three colonies for each transformant were grown at 37 °C, shaking at 180 rpm to an OD_{600} of 0.3 in 2xLB or 2xLB supplemented with 300 mM acetate, 290 mM glycerol, 40 μM pantethine, and 16 μM biotin before the MGS synthesis was induced with 1 mM IPTG and 0.2% L-arabinose. At different time points, the OD_{600} of 1 mL culture was measured prior to cell pelleting, and cells were concentrated by resuspending them in 200 μL of buffer G (50 mM Tris, 200 mM NaCl, 15 mM EDTA). GFP fluorescence was measured (488 nm excitation−512 nm emission) using a Spectramax GEMINI EM microplate reader (Molecular Devices) and normalized by the corresponding OD_{600} value.

RESULTS

MGS Binds Anionic Lipids Selectively. Tightly associated membrane lipids are known to follow transmembrane proteins into their 3D crystals[31] and stay adherent during detergent solubilization and purification. To investigate whether any lipids tightly associates with MGS, we used a "mild" extraction process for MGS and two inactive mutants, E300A and E308A. Membranes were solubilized by 2 mM dodecylmaltoside (DDM), a condition known to preserve all major inner membrane protein complexes from *E. coli*.[32] This procedure revealed that MGS had three kinds of endogenous lipids associated with it (Figure 2B): the anionic PG and CL but intriguingly also its own enzymatic product α-monoglucosyldiacylglycerol (GlcDAG).[33] As expected, no GlcDAG lipids were detected on either of the inactive mutants, which equally well induce vesicle formation in *E. coli* when overexpressed.[13] Remarkably, zwitterionic PE lipids, the major species in membranes of *E. coli* cells,[13] were not found to be present on the purified MGS (or the mutants). The presence of the "foreign" GlcDAG seems logical, given that this membrane lipid is the major species in the MGS native host *Acholeplasma laidlawii*,[34] but also indicates a binding preference for GlcDAG versus e.g. PE. The two inactive mutants contained as expected no GlcDAG, but also here no PE could be detected on the proteins. A validation of the lipid analysis method was performed with a DDM extract from labeled BL21 AI cells with no MGS present, which revealed no lipids bound to the affinity resin, supporting the finding that the detected lipids were copurified only with MGS.

The number of MGS-associated lipid molecules was estimated by quantifying lipid spot radioactivity, together with the relationships between OD_{600} and cell culture volumes[35,36] and using data in the CyberCell database. This procedure revealed that MGS contained 3.3 PG, 0.3 CL, and 5.2 GlcDAG molecules per protein. The inactive E300A mutant protein contained 1.4 PG, 0.6 CL, and 0 GlcDAG, and the E308A variant had 2.7 PG, 1.4 CL, and 0 GlcDAG molecules per protein. Somewhat surprisingly, the two mutants differed in their lipid-binding capacities, and only around 2 lipid molecules in total bound to the E300A mutant, while the E308A mutant bound to around 4 lipids and on average to more CL than the other proteins. These differences could in part be explained by their different abilities to bind to the substrate (UDP-Glc), which in turn may have an impact on the conformation, and thus lipid-binding properties, of the proteins. From these results we conclude that MGS binds the anionic lipids PG and CL with a tight association and that the lack of GlcDAG in inactive MGS mutants does not induce binding of other lipids to the protein. Since PG and CL lipids are minority lipids in the *E. coli* membrane, this observation establishes a preferential binding of MGS to anionic lipids *in vivo*.

^{31}P NMR Studies of MGS−Lipid Binding in Bicelles. The selective binding of MGS to *E. coli* lipids was tested *in vitro* by using ^{31}P NMR with bicelles prepared with purified lipids from native *E. coli* membranes and lipid-free MGS obtained with the detergent-free purification protocol. Two bicelle mixtures were used: one with and one without GlcDAG (+GlcDAG and −GlcDAG bicelles, respectively).

For both −GlcDAG bicelles and +GlcDAG bicelles, four peaks were observed in 1D ^{31}P NMR spectra. They originate from the phosphorus in PG, CL, PE, and DHPC (Figure 3). To verify that the natural lipids were incorporated into bicelles, we used ^{31}P pulsed field gradient diffusion NMR to measure the relative size of +GlcDAG bicelles. The amount of CL was too low to allow for accurate measurements of diffusion coefficients, but the diffusion coefficients for PE and PG as well as DHPC could be reliably evaluated. Both PE and PG had diffusion coefficients of around 5×10^{-11} m^2 s^{-1} [$(5.3 \pm 0.5) \times 10^{-11}$ m^2 s^{-1} for PG and $(4.8 \pm 0.4) \times 10^{-11}$ m^2 s^{-1} for PE] which strongly supports that they are located in the same type of lipid aggregates. The faster diffusion of DHPC [$(11.7 \pm 0.6) \times 10^{-11}$ m^2 s^{-1}] indicates that not all of the DHPC molecules take part in bicelle formation, as noted earlier.[37,38] The diffusion coefficients can be related to hydrodynamic dimensions through the Stokes−Einstein relationship,[39] and the data for the *E. coli* bicelles indicate an apparent hydrodynamic radius of around 3.9−4.2 nm, in agreement with bicelles made with other and similar lipids.[40,41] Hence, we conclude that the *E. coli* lipid mixture forms small fast-tumbling bicelles.

To investigate the effect that MGS had on the different lipids, and thus to provide insight into specific lipid interactions, 1D ^{31}P NMR spectra were recorded for bicelles as a function of increasing MGS concentration (Figure 3). Increasing the amount of MGS in both bicelle samples caused significant decreases of peak intensities and line broadening. In both lipid mixtures, the intensities of the CL, PG, and PE peaks decreased severely and the line widths increased significantly upon adding MGS (Figure 3B). Moreover, the PG and CL chemical shifts changed gradually and consistently with increasing MGS concentrations in both types of bicelles, while the chemical shift changes for PE and DHPC were much smaller and not consistent in sign over the protein concentration range. No differences between the two bicelles, −GlcDAG and +GlcDAG, could be observed. These results indicate a preferential interaction between MGS and the anionic lipids, PG and CL.

dx.doi.org/10.1021/bi400616n | *Biochemistry* 2013, 52, 5533−5544

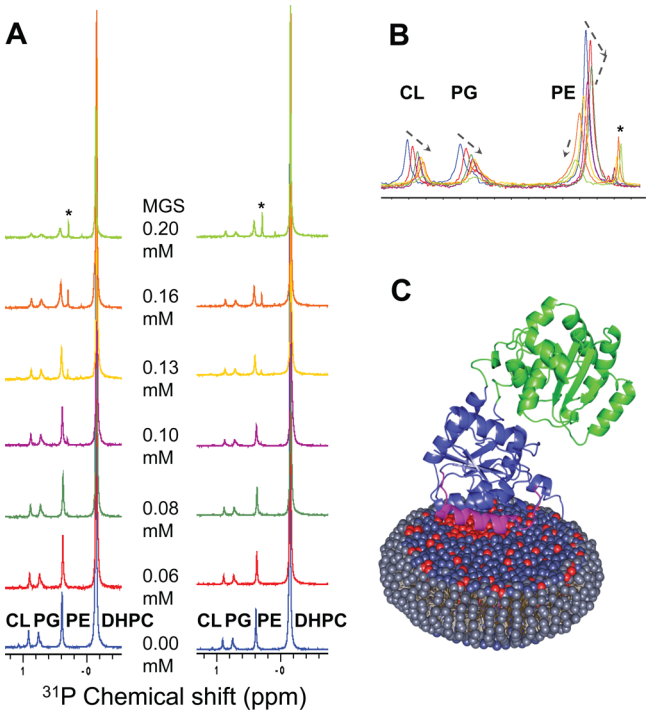

Figure 3. ^{31}P NMR investigation of MGS–lipid interaction. (A) ^{31}P NMR spectra of bicelles containing *E. coli* lipids:DHPC (25:50 mM) with increasing amounts of MGS recorded at 25 °C. On the left are spectra for −GlcDAG bicelles and on the right are spectra for +GlcDAG bicelles. (B) Overlayed spectra zoomed in for −GlcDAG bicelles with different MGS concentrations. The star indicates a peak that appeared with the addition of MGS. (C) Schematic representation of bicelles made up of anionic lipids (red, PG and CL), zwitterionic lipids (blue, PE), and short-chained lipids (gray, DHPC) with bound MGS. The two Rossmann fold domains in MGS are indicated in green and blue, respectively, with a putative binding helix indicated in magenta.

The lower ^{31}P chemical shifts experienced by both anionic lipids in the presence of MGS may indicate a change in membrane surface charge. Previous studies have shown that isotropic ^{31}P shifts drop as a function of decreased negative bilayer surface charge.[42] Hence, the results indicate less negative charge on the bicelle surface, induced by binding of positively charged regions of MGS. A cartoon of this binding is provided in Figure 3C.

The MGS–lipid binding was further investigated by measuring longitudinal and transverse relaxation time constants, T_1 and T_2, for each lipid phosphate in the absence and presence of MGS (Table S1, Supporting Information). T_1 is typically affected by relatively fast local motions of individual lipid molecules or of bond vectors within a molecule, while T_2, in addition to the fast motions, is greatly affected by the much slower overall tumbling of the entire bicelle.[38,43] A large difference between T_1 (0.65–0.73 s) and T_2 (0.05–0.11 s) values measured for each lipid was observed, indicating that the slow, overall motion of the bicelle strongly influences the T_2 relaxation of the lipids. Only minor differences in T_1 and T_2 values recorded for lipids in −GlcDAG bicelles and +GlcDAG bicelles in the absence of MGS were seen, indicating a similar behavior of the lipids in the two bicelles. Adding MGS had none or limited effects on T_1 relaxation, but in contrast to this, MGS decreased the T_2 relaxation time constants for all lipids (including DHPC) in the −GlcDAG bicelles by around 20%, while no significant effect was observed for the lipids in +GlcDAG bicelles. This result indicates that MGS binds to −GlcDAG bicelles and +GlcDAG bicelles in different ways, possibly affecting the size of the bicelles.

A new sharp peak next to the PE peak appeared and increased in intensity upon adding MGS. The integrated intensity indicated that it is only a minor amount and most likely originates from a degradation product from one of the lipids. We noted that the new sharp peak had much slower relaxation behavior than the lipids, with T_1 in the range 1.2–1.4 s and T_2 between 0.5 and 0.7 s, supporting the conclusion of a small degradation product. To confirm that no phospholipids or other phosphorus-containing molecules were introduced with the addition of MGS, a ^{31}P spectrum of 0.2 mM MGS solution (the highest concentration used in the titration series) was recorded, and no traces of a ^{31}P signal could be detected.

We conclude from the NMR results that MGS can bind to both types of bicelles, that anionic lipids (PG and CL) are mostly affected by MGS binding, and that MGS binds to bicelles in different ways if GlcDAG is present or not. The presence of GlcDAG in the bicelles decreases the effect that the enzyme has on anionic lipid mobility somewhat, supporting once more the conclusion of a specific interaction between GlcDAG and MGS.

Stimulation of Phospholipid Synthesis Correlates with MGS Overexpression. A complex and rich growth medium, like TB, yields higher membrane quantities and thus greatly contributes to higher overexpression levels of proteins. TB is a rich combination of tryptone and yeast extract that contains carbon sources, cofactors, vitamins, and precursors required for the synthesis of phospholipids and proteins.[44−48] To examine the effect of individual important lipid precursors, supplementation of four factors, one by one, or in combination, to normal LB medium were tested (Figure 4): pantethine, a precursor to CoA; biotin, an essential cofactor for the acetyl-CoA carboxylase in fatty acid synthesis; and finally glycerol[45] and acetate,[46] both important carbon sources for lipid synthesis.

The most effective concentrations for the simultaneous *in situ* combinations of all four lipid precursors/cofactors with respect to lipid and MGS quantities *in vivo* were assayed by an experimental design approach (Figure 4 and Table S2, Supporting Information), where a maximum amount of information from a minimum number of combinatorial experiments could be obtained. The input variables in the experimental design were the concentrations of acetate, glycerol, biotin, and pantethine, and the response variables were the amounts of MGS protein and the amounts of synthesized PE, PG, CL, and GlcDAG lipids.

Figures 4A and 4B show the amount of synthesized membrane lipids produced under these varying conditions, together with MGS amounts. The TLC analysis showed that all supplements were able to stimulate the amount of lipids synthesized in BL21 AI-MGS cells but to various extents, but yielded only minor effects in the BL21 AI control strain without MGS (data not shown). For example, a nearly 3-fold increase in protein content per OD_{600} unit for the BL21 AI-MGS cells was observed in the presence of 60 mM acetate compared to BL21 AI cells.

Figure 4C shows a histogram of the amount of produced MGS together with the total lipid production as a function of acetate concentration (from low to high), which shows a remarkable correlation between low acetate and low MGS/lipid production and, correspondingly, between high acetate and

dx.doi.org/10.1021/bi400616n | *Biochemistry* 2013, 52, 5533−5544

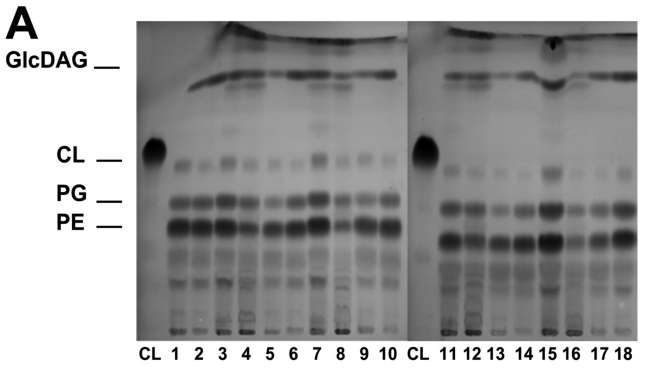

CONDITIONS		EXPERIMENT NUMBER																
Supplement	Concentration	10	9	5	6	1	2	13	14	17	18	7	3	15	11	8	4	12	16
Acetate	L: 12 mM M: 150 mM H: 300 mM	L	L	L	L	L	L	L	L	M	M	H	H	H	H	H	H	H	H
Glycerol	L: 0 mM M: 145 mM H: 290 mM	L	H	L	H	L	H	L	H	M	M	L	L	L	L	H	H	H	H
Pantethine	L: 20 μM M: 30 μM H: 40 μM	H	H	L	L	L	L	H	H	M	M	L	L	H	H	L	L	H	H
Biotin	L: 8 μM M: 12 μM H: 16 μM	L	L	H	H	L	L	H	H	M	M	H	L	H	L	H	L	L	H

Figure 4. Stimulation of phospholipid synthesis in LB results in increased expression levels of MGS. Lipid precursors and cofactors (indicated in Figure 1) were jointly evaluated by an experimental design approach described in Table S2. (A) TLC analysis of extracted lipids from BL21-AI MGS cells grown with the supplemented conditions decided by the design. (B) Western blots visualizing MGS amounts for the same set of conditions as for the lipid analyses. (C) Histogram indicating the protein and lipid responses, in absorbance units (AU, from imager software), per OD_{600} unit (after normalization). Responses were ranked according to the strong increment in lipid and MGS amounts per OD_{600} unit. The indications for low (L), medium (M), and high (H) concentrations for each lipid precursor/cofactor tested are given in the left corner of the text table.

high MGS/lipid production. For the high acetate conditions (300 mM, i.e., samples 15, 11, 8, 4, 12, and 16, in Figure 4C), the impact of glycerol, pantethine, and biotin was also evident both for lipid and MGS amounts synthesized, while at low acetate concentrations, the effect of the other supplements was marginal. We therefore conclude that acetate appeared to be most significant for the production of both protein and lipids, while the other factors modulate the synthesis under high acetate conditions.

Partial least-squares (PLS) analyses of the response data revealed that synthesized MGS protein amounts were often strongly correlated with the amounts of synthesized phospholipids, yielding good PLS models as indicated by the quality measures R2 and Q2 (Figure S1, Supporting Information). Among the four supplements jointly tested, acetate had the highest contribution to both phospholipid synthesis and overexpression of MGS, while pantethine and biotin had a negligible effect on the synthesis of any of the lipids or MGS, in agreement with the direct experimental observations. Moreover, it was observed that the synthesis of PG was more strongly correlated with acetate than the synthesis of the other lipids or MGS (Figure 5). In fact, a combination of high

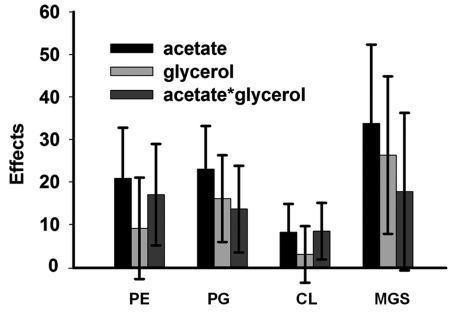

Figure 5. PLS analyses of the correlation between acetate/glycerol levels, production of different lipid species, and MGS. Acetate is indicated by black bars, glycerol by light gray bars, and acetate + glycerol by dark gray bars. Negative error bars indicate a noncorrelated relationship between variables and responses while positive error bars show a good correlation.

acetate/glycerol levels correlated with an increase in PG and MGS, but not with PE and CL amounts. This is a significant finding since PG is the direct precursor to CL in the lipid synthesis pathway (Figure 1) and is considered to be a pacekeeper for *E. coli* membrane lipid synthesis.[17] Foremost, the PLS analysis highlighted that the contribution of acetate was not only to PG synthesis but also to MGS production. Hence, a tight coupling between MGS production and lipid production was revealed.

Incorporation of Acetate in Lipids Studied by FT-IR. The possible correlation between stimulation of phospholipid synthesis and increased MGS production was also studied by Fourier transform infrared spectroscopy (FT-IR). Figure 6 displays infrared spectra recorded from intact cells (Figure 6A,B) and membrane lipid extracts (Figure 6C,D). The quantification of lipids (Figure 6E) was based on integration of the C═O band at 1740 cm^{-1},[49−51] while protein content was monitored by integration of the amide I band at 1654 cm^{-1}. Our data indicated a 2-fold increase in phospholipid production (C═O band at 1740 cm^{-1}) in BL21 AI-MGS cells with added acetate, which brought about a 2.8-fold induction of MGS production (Figure 6E), supporting a coupling between lipid synthesis and MGS overexpression. A much smaller stimulatory effect of acetate on lipid production was observed for BL21 AI cells without MGS, accentuating a significant role of MGS for stimulating phospholipid synthesis. The protein content in the cells without MGS was not affected by acetate.

The level of incorporation of ^{2}H-labeled acetate into fatty acids was also monitored. Figures 6C,D show FT-IR spectra of the lipid extracts. The spectra give evidence for the incorporation of the deuterated acetate into lipids, since CD stretching vibrations are observed in the 2000−2200 cm^{-1} region.[52,53] The band positions are 2241 (shoulder), 2215, 2138, and 2075 cm^{-1}. They are different from the positions of

dx.doi.org/10.1021/bi400616n | *Biochemistry* 2013, 52, 5533−5544

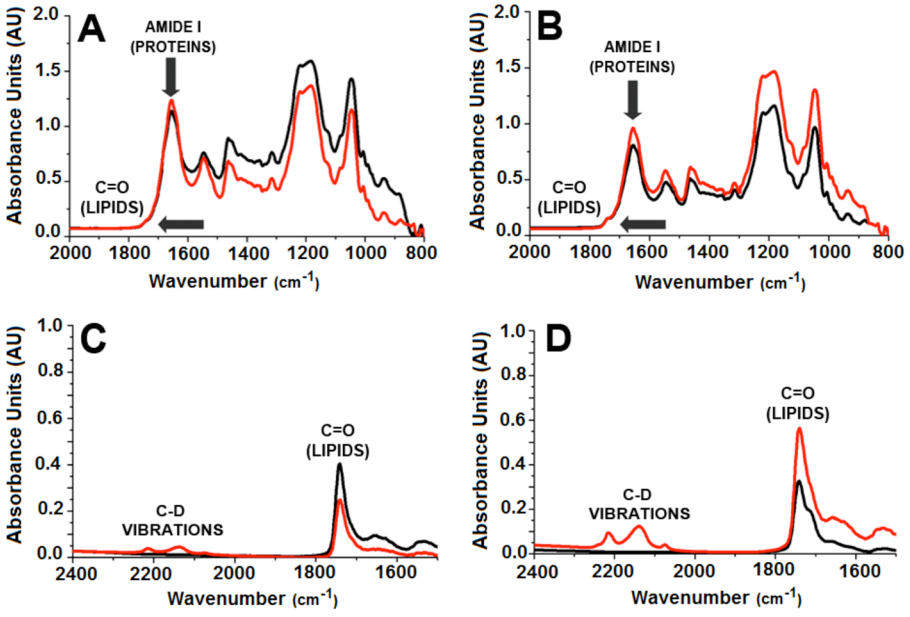

E

SPECTRA		INTEGRATIONS Measured value x Dilution factor = Real value	
		Amide I band (Proteins)	C=O band (Lipids)
A	Non-acetate	4.38x2=8.76	0.027x2=0.054
	Acetate	4.45x2=8.9	0.036x2=0.072
B	Non-acetate	3.53x4=14.14	0.03x4=0.12
	Acetate	4.058x10=40.58	0.028x10=0.28

Figure 6. Examination of protein and lipid quantities by FT-IR analysis. All spectra were taken under normalized conditions with same OD_{600} units. (A) Intact BL21-AI cells (without MGS); (B) intact BL21AI-MGS cells (with MGS); (C) membrane lipid extracts (chloroform phase) from BL21-AI cells; and (D) from BL21-AI MGS cells. Black curves indicate LB medium under nonacetate conditions, and red curves represent cells or lipids grown in LB medium supplemented with 300 mM deuterated acetate (C^2H_3COONa). Note the unique C−D vibrations in lipids from the deuterated acyl chains. (E) Band integrations for (A) control and (B) MGS vesicle cells. These values are band absorbances compensated for dilutions made prior to analysis.

the CD_3 bands of acetate (2255 and 2231 cm^{-1}), and the observed signals are assigned to acyl groups synthesized from deuterated acetate. The observed band positions are different from those expected for fully deuterated acyl chains[52,53] and for most selectively deuterated CD_2 groups in otherwise undeuterated chains[54−56] but coincide with the band positions of CD_2 groups next to the ester group (2′-position) and of CD_3 groups, which are typically found near 2210, 2120, and 2075 cm^{-1}.[55−57] The former band is the strongest and was assigned to the asymmetric stretching vibration. The latter bands are weaker and both assigned to a Fermi resonance doublet between the symmetric stretching vibration and an overtone or combination band. The band near 2120 cm^{-1} is was much weaker than expected for fully deuterated moieties. Hence, fully deuterated methyl or 2′-methylene groups alone are insufficient to explain our spectra. Singly labeled methylene groups, CHD, absorb in the same spectral range,[54,58] near 2140 cm^{-1}, and singly labeled methyl groups CH_2D are also expected to absorb here. We conclude that the deuterated methyl group of acetate was incorporated at the beginning and/or the end of the acyl chains and that the deuterium was further incorporated into singly labeled methyl or methylene groups. From the band areas of the CH and CD vibrations, the percentage of incorporation of deuterium was estimated to be around 20% for MGS-containing cells and 10% for cells without MGS. The larger incorporation of deuterium in the MGS cells is in agreement with a stronger stimulation of lipid synthesis by acetate.

In summary, the results indicated that addition of acetate to the growth media resulted in ∼2 times stimulation of phospholipid synthesis in MGS containing BL21 AI-MGS cells, compared to BL21 AI cells, providing evidence for a coupling between lipid synthesis and protein overexpression levels, in agreement with the MVDA analyses.

Involvement of Envelope Stress Response. Bacteria have a number of regulon networks for control and responses to various types of environmental, metabolic, and stress conditions. For membrane envelope stress, the sigma^E (σ^E) and Cpx systems are acknowledged as the most significant stress systems activated when cells are subjected to various stressors.[59−64] Several enzymes employed in phospholipid synthesis[60] in *E. coli* are involved in the σ^E system, encoded by the rpoE gene, which also has a certain overlap with another stress regulon system, the Cpx. A promoter activity assay that utilizes GFP fusions to the promoter of the rpoE gene was used to investigate the possibility of a stress response to the stimulation of lipid production. In addition, promoters of genes involved in the lipid synthesis, plsB, cfa, and psD were also tested.

BL21 AI (without MGS) and/or BL21 AI-MGS (with MGS) transformants were analyzed with the supplements described above (glycerol, acetate, biotin, and pantethine). Only modestly increased ratios between the signals (GFP fluorescence)

dx.doi.org/10.1021/bi400616n | *Biochemistry* 2013, 52, 5533−5544

detected for the supplemented condition compared to the normal one were observed (Figure 7), indicating only minor

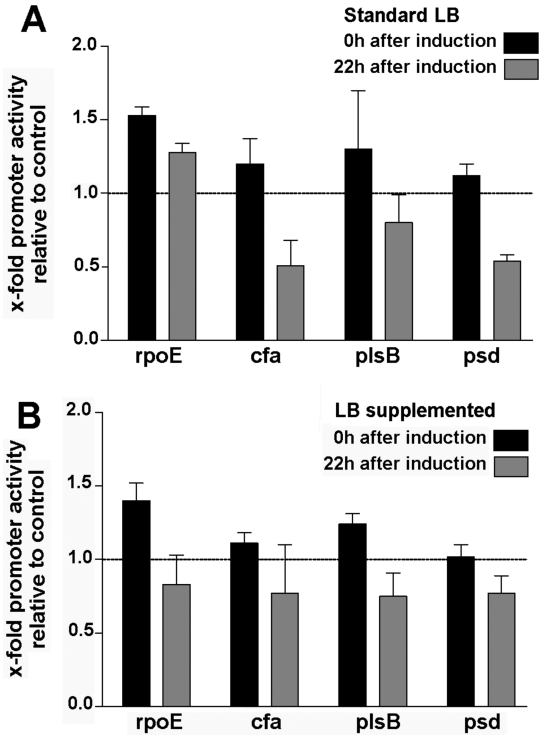

Figure 7. Expression of selected genes for envelope stress (rpoE) or lipid biosynthesis (cfa, plsB, and psD) in *E. coli* BL21 AI-MGS cells relative to *E. coli* BL21 AI cells. The expression levels were monitored by measuring the fluorescence signal from promoter-GFP fusions. Black bars represent the time point directly after induction of MGS synthesis, and gray bars represent the expression pattern after 22 h of induction. (A) Expression patterns in standard LB medium. (B) Expression patterns in LB supplemented with acetate, glycerol, biotin, and pantethine.

changes in the regulation of these reporter genes. Initially a modest σ^E stress as indicated by a small increase in rpoE (×1.5) levels was observed for BL21 AI-MGS cells, which was probably caused by the overexpression of a foreign protein (MGS) in *E. coli*, but this increase must be considered as minor (Figure 7). 22 h after induction, transcription levels were fairly similar with and without supplements. Overall, we conclude that the supplemented LB seems not to influence the transcription levels of any of the tested genes significantly and that the RpoE stress responses are not significantly up-regulated in the presence of MGS and during increased lipid synthesis.

DISCUSSION

A number of foreign and endogenous membrane proteins can generate extra intracellular membranes when overexpressed in *E. coli*, and they are also known to preserve certain phospholipids on their structure during purification.[5,6,13,15] The monotopic GT MGS is one such protein, which has several membrane-interacting segments and many positively charged residues (pI 9.5), including a number of charged amino acid residue pairs.[20] The number of copurified lipids detected on MGS was here observed to be higher than what has earlier been asserted for a structurally very similar *E. coli* GT protein, LpxB in LPS synthesis, which showed maximally 3.5 mol of a PE/PG/CL mixture per mole of LpxB, of which the majority were PE molecules.[5] The membrane-associated GT, MurG, was also found to accommodate mainly PE,[6] while here we found no PE binding to MGS. Moreover, aside from the enzymatic product, GlcDAG, MGS, as well as the inactive mutants, bound only to anionic lipids (PG and CL). This *in vivo* selective binding was supported by ^{31}P NMR experiments in model systems. MGS has an amphipathic helix of alternating hydrophobic and positively charged residues on its surface, which is known to be important for membrane insertion,[18,65] while other GTs like MurG[6] and LpxB[5] bear less positive charges and generate less internal vesicles in *E. coli* than MGS.[13] Thus, the strength of interaction with anionic lipids and the ability to stimulate lipid synthesis appear to be correlated.

The amount of lipids bound to MGS represents the withdrawal of at most ∼5% of the total amount of polar lipids present in the cell. Among the lipid molecules detected on MGS, PG was the most retained lipid species. For *E. coli* lipid metabolism, PG seems to be a "pace-keeper" for lipid synthesis,[18] which also sets the large *in vivo* PE amounts by a charge-density regulatory mechanism. Here, a selective interaction between anionic lipids and MGS was proven to exist, and this sequestering of anionic lipids by MGS seems to stimulate lipid synthesis, as shown by the higher lipid content of MGS overexpressing cells. The addition of lipid precursors and cofactors stimulates the activity of all lipid synthases, thus increasing the total lipid production in the cell. A correlation between total lipid synthesis and MGS production was clearly observed here, as higher lipid levels induced by the addition of lipid precursors gave rise to a higher MGS overexpression (Figure 4C). This observation was evidenced by MVDA (Figure 5) and FT-IR (Figure 6) analyses of the correlation between lipid synthesis, MGS overexpression, and the addition of supplements. Acetate was observed to have a large impact on the amount of synthesized lipids, however, only in the presence of MGS. Increased lipid synthesis has also been observed for inactive MGS mutants,[13] indicating that it is not the enzymatic activity of the protein that affects lipid production but instead the binding of anionic lipids most likely plays a key role. This strongly suggests the presence of one or several signaling mechanism(s) connected to anionic lipids. This indicates that even though the actual numbers of anionic lipids that are withdrawn by MGS is minor, a signaling mechanism through anionic lipids would allow for the creation of more membrane surface for MGS to bind in a "feed-forward" manner (Figure 1).

Even though acetate was observed to stimulate lipid synthesis in MGS cells, the majority of the lipids are still made from peptides/amino acids in the LB medium. This result indicates that acetate does not only contribute as a precursor, but in fact contributes to a much larger increase in lipid production. The end product of the fatty acid synthesis, acyl-ACP, is a key regulator for lipid synthesis, and the level of this molecule is controlled by the G3P-acyltransferase, PlsB.[30,66−68] PlsB gene transcription is in turn affected by rpoE in the "envelope stress" system. The up-regulation of the lipid synthesis pathway is not a normal phenomenon for *E. coli* membranes, but the stress response system appears to remain inactivated during over-stimulation of lipid synthesis. The relief of stress caused by the higher lipid production is instead taken care of by forming intracellular vesicles.

In conclusion, we have shown that a strong correlation between increased membrane lipid synthesis, promoted by the addition of lipid precursors and cofactors, and MGS expression exists. Essentially no increase in lipid synthesis occurred in the

dx.doi.org/10.1021/bi400616n | *Biochemistry* 2013, 52, 5533−5544

absence of MGS, which supports the conclusion that MGS stimulates *E. coli* to synthesize more lipids, in a "feed-forward" manner. Moreover, the enzymatic activity of the protein does not appear to be important. MGS, as well as the inactive variants, binds selectively to anionic lipids, which most likely is a part of a signaling mechanism for lipid synthesis. The creation of more membranes allows for binding of more MGS molecules, which relieves the membrane tension created by the incorporation of massive amounts of newly synthesized proteins into the inner membranes of *E. coli*. An additional factor for the up-regulation of the lipid pathway may be related to the decrease in the lipid surface charge density due to the binding of many overall positively charged MGS molecules to anionic lipids. This decrease in surface charge is also sensed by the lipid-synthesizing machinery leading to an increase in anionic lipid synthesis, which also up-regulates PE production, and therefore the total amount of lipids.

■ ASSOCIATED CONTENT

Supporting Information

Relaxation data (T_1 and T_2) for ^{31}P in *E. coli* lipid bicelles (Table S1); experimental design composition table showing the various concentrations of lipid precursors (cofactors and building blocks) for membrane lipid synthesis jointly tested with multivariate data analysis (Table S2); illustration of the linearity of MVDA analysis for experimental design outputs (Figure S1). This material is available free of charge via the Internet at http://pubs.acs.org.

■ AUTHOR INFORMATION

Corresponding Author

*Tel (+46)-8-162487, Fax (+46)-8-153679, e-mail candan@dbb.su.se (C.A.); Tel (+46)-8-162448, Fax (+46)-8-155597, e-mail lena.maler@dbb.su.se (L.M.).

Funding

This research was supported by grants from the Swedish Foundation for Strategic Research (SSF) to the Center for Biomembrane Research (CBR), the Carl Trygger Foundation, and from the Swedish Research Council. The FT-IR and NMR spectrometers were funded by Knut and Alice Wallenbergs Stiftelse.

Notes

The authors declare no competing financial interest.

■ ACKNOWLEDGMENTS

The authors thank Dr. Daniel Daley for sharing his *E. coli* integral membrane protein collection with promoter plasmids and Dr. Saroj Kumar for discussions concerning FT-IR measurements.

■ DEDICATION

We would like to commemorate Prof. Åke Wieslander, who sadly passed away during the final stages of completing this work. We are in a tremendous grief but will always remember him for his great personality and for being a devoted scientist and most importantly a good-spirited friend.

■ ABBREVIATIONS

DHPC, 1,2-dihexanoyl-*sn*-glycero-3-phosphocholine; CFA, cyclopropane fatty acid synthase; CL, cardiolipin; *Escherichia coli*, *E. coli*; FT-IR, Fourier transformed infrared spectroscopy; GlcDAG, monoglucosyldiacylglycerol; GT, glycosyltransferase; LB, Luria−Bertani broth; LpxB, Lipid A disaccharide synthase; MGS, monoglucosyldiacylglycerol synthase; MVDA, multivariate data analysis; NMR, nuclear magnetic resonance; PE, phosphatidylethanolamine; PG, phosphatidylglycerol; PLS, partial least-squares; PlsB, G3P-acyltransferase; PM, plasma membrane; PSD, phosphatidylserine decarboxylase; TB, Terrific Broth; TLC, thin layer chromatography.

■ REFERENCES

(1) Phillips, R., Ursell, T., Wiggins, P., and Sens, P. (2009) Emerging roles for lipids in shaping membrane-protein function. *Nature 459*, 379−385.

(2) Cronan, J. E. (2003) Bacterial membrane lipids: Where do we stand? *Annu. Rev. Microbiol. 57*, 203−224.

(3) Miller, K. R. (1979) Structure of a bacterial photosynthetic membrane. *Proc. Natl. Acad. Sci. U. S. A. 76*, 6415−6419.

(4) Wilkison, W., Bell, R., Taylor, K., and Costello, M. (1992) Structural characterization of ordered arrays of sn-glycerol-3-phosphate acyltransferase from *Escherichia coli*. *J. Bacteriol. 174*, 6608−6616.

(5) Metzger, L. E., IV, and Raetz, C. R. (2009) Purification and characterization of the lipid A disaccharide synthase (LpxB) from *Escherichia coli*, a peripheral membrane protein. *Biochemistry 48*, 11559−11571.

(6) van den Brink-van der Laan, E., Boots, J. P., Spelbrink, R. E., Kool, G. M., Breukink, E., Killian, J. A., and de Kruijff, B. (2003) Membrane interaction of the glycosyltransferase MurG: A special role for cardiolipin. *J. Bacteriol. 185*, 3773−3779.

(7) Lemire, B. D., Robinson, J. J., Bradley, R. D., Scraba, D. G., and Weiner, J. H. (1983) Structure of fumarate reductase on the cytoplasmic membrane of *Escherichia coli*. *J. Bacteriol. 155*, 391−397.

(8) Weiner, J. H., Lemire, B. D., Elmes, M. L., Bradley, R. D., and Scraba, D. G. (1984) Overproduction of fumarate reductase in *Escherichia coli* induces a novel intracellular lipid-protein organelle. *J. Bacteriol. 158*, 590−596.

(9) Elmes, M. L., Scraba, D. G., and Weiner, J. H. (1986) Isolation and characterization of the tubular organelles induced by fumarate reductase overproduction in *Escherichia coli*. *J. Gen. Microbiol. 132*, 1429−1439.

(10) Vergères, G., Yen, T. S. B., Aggeler, J., Lausier, J., and Waskell, L. (1993) A model system for studying membrane biogenesis. Overexpression of cytochrome b5 in yeast results in marked proliferation of the intracellular membrane. *J. Cell Sci. 106*, 249−259.

(11) Arechaga, I., Miroux, B., Karrasch, S., Huijbregts, R., de Kruijff, B., Runswick, J., and Walker, J. E. (2000) Characterization of new intracellular membranes in *Escherichia coli* accompanying large scale over-production of the b subunit of F_1F_0 ATP synthase. *FEBS Lett. 482*, 215−219.

(12) Graham, T. R., and Kozlov, M. M. (2010) Interplay of proteins and lipids in generating membrane curvature. *Curr. Opin. Cell Biol. 22*, 430−436.

(13) Eriksson, H. M., Wessman, P., Ge, C., Edwards, K., and Wieslander, Å. (2009) Massive formation of intracellular membrane vesicles in *Escherichia coli* by a monotopic membrane-bound lipid glycosyltransferase. *J. Biol. Chem. 284*, 33904−33914.

(14) Eriksson, H. M., Persson, K., Zhang, S., and Wieslander, Å. . (2009) High-yield expression and purification of a monotopic membrane glycosyltransferase. *Protein Expr. Purif. 66*, 143−148.

(15) Ha, S., Walker, D., Shi, Y., and Walker, S. (2000) The 1.9 Å crystal structure of *Escherichia coli* MurG, a membrane-associated glycosyltransferase involved in peptidoglycan biosynthesis. *Protein Sci. 9*, 1045−1052.

(16) Edman, M., Berg, S., Storm, P., Wikström, M., Vikström, S., Öhman, A., and Wieslander, Å. (2003) Structural features of glycosyltransferases synthesizing major bilayer and nonbilayer-prone membrane lipids in *Acholeplasma laidlawii* and *Streptococcus pneumoniae*. *J. Biol. Chem. 278*, 8420−8428.

(17) Jackson, B. J., Gennity, J., and Kennedy, E. (1986) Regulation of the balanced synthesis of membrane phospholipids. Experimental test of models for regulation in *Escherichia coli*. *J. Biol. Chem. 261*, 13464−13468.
(18) Linde, K., Gröbner, G., and Rilfors, L. (2004) Lipid dependence and activity control of phosphatidylserine synthase from *Escherichia coli*. *FEBS Lett. 575*, 77−80.
(19) Li, L., Storm, P., Karlsson, O. P., Berg, S., and Wieslander, Å. (2003) Irreversible binding and activity control of the 1, 2-diacylglycerol 3-glucosyltransferase from *Acholeplasma laidlawii* at an anionic lipid bilayer surface. *Biochemistry 42*, 9677−9686.
(20) Lind, J., Rämö, T., Klement, M. L. R., Bárány-Wallje, E., Epand, R. M., Epand, R. F., Mäler, L., and Wieslander, Å. (2007) High cationic charge and bilayer interface-binding helices in a regulatory lipid glycosyltransferase. *Biochemistry 46*, 5664−5677.
(21) Bligh, E., and Dyer, W. J. (1959) A rapid method of total lipid extraction and purification. *Can. J. Biochem. Phys. 37*, 911−917.
(22) Vold, R. R., Prosser, R. S., and Deese, A. J. (1997) Isotropic solutions of phospholipid bicelles: A new membrane mimetic for high-resolution NMR studies of polypeptides. *J. Biomol. NMR 9*, 329−335.
(23) Marcotte, I., and Auger, M. (2005) Bicelles as model membranes for solid-and solution-state NMR studies of membrane peptides and proteins. *Concepts Magn. Reson., Part A 24*, 17−37.
(24) Warschawski, D. E., Arnold, A. A., Beaugrand, M., Gravel, A., Chartrand, É., and Marcotte, I. (2011) Choosing membrane mimetics for NMR structural studies of transmembrane proteins. *Biochim. Biophys. Acta 1808*, 1957−1974.
(25) Mäler, L., and Gräslund, A. (2009) Artificial membrane models for the study of macromolecular delivery. *Methods Mol. Biol. 480*, 129−139.
(26) Mäler, L. (2012) Solution NMR studies of peptide-lipid interactions in model membranes. *Mol. Membr. Biol. 29*, 1−22.
(27) Stejskal, E. O., and Tanner, J. E. (1965) Spin diffusion measurements: Spin echoes in the presence of a time dependent field gradient. *J. Chem. Phys. 42*, 288−292.
(28) von Meerwall, E., and Kamat, M. (1989) Effect of residual field gradients on pulsed gradient NMR diffusion measurements. *J. Magn. Reson. 83*, 309−323.
(29) Nolin, B., and Jones, R. N. (1953) The infrared absorption spectra of diethyl ketone and its deuterium substitution products. *J. Am. Chem. Soc. 75*, 5626−5628.
(30) Wahl, A., My, L., Dumoulin, R., Sturgis, J. N., and Bouveret, E. (2011) Antagonistic regulation of dgkA and plsB genes of phospholipid synthesis by multiple stress responses in *Escherichia coli*. *Mol. Microbiol. 80*, 1260−1275.
(31) Palsdottir, H., and Hunte, C. (2004) Lipids in membrane protein structures. *Biochim. Biophys. Acta 1666*, 2−18.
(32) Stenberg, F., Chovanec, P., Maslen, S. L., Robinson, C. V., Ilag, L. L., von Heijne, G., and Daley, D. O. (2005) Protein complexes of the *Escherichia coli* cell envelope. *J. Biol. Chem. 280*, 34409−34419.
(33) Berg, S., Edman, M., Li, L., Wikström, M., and Wieslander, Å. (2001) Sequence properties of the 1, 2-diacylglycerol-3-glucosyl-transferase from *Acholeplasma laidlawii* membranes recognition of a large group of lipid glycosyltransferases in eubacteria and archaea. *J. Biol. Chem. 276*, 22056−22063.
(34) Wieslander, Å., Nordström, S., Dahlqvist, A., Rilfors, L., and Lindblom, G. (1995) Membrane lipid composition and cell size of acholeplasma laidlawii strain A are strongly influenced by lipid acyl chain length. *Eur. J. Biochem. 227*, 734−744.
(35) Sezonov, G., Joseleau-Petit, D., and D'Ari, R. (2007) *Escherichia coli* physiology in Luria-Bertani broth. *J. Bacteriol. 189*, 8746−8749.
(36) Volkmer, B., and Heinemann, M. (2011) Condition-dependent cell volume and concentration of *Escherichia coli* to facilitate data conversion for systems biology modeling. *PLoS One 6*, e23126.
(37) Glover, K. J., Whiles, J. A., Wu, G., Yu, N., Deems, R., Struppe, J. O., Stark, R. E., Komives, E. A., and Vold, R. R. (2001) Structural evaluation of phospholipid bicelles for solution-state studies of membrane-associated biomolecules. *Biophys. J. 81*, 2163−2171.
(38) Andersson, A., and Mäler, L. (2005) Magnetic resonance investigations of lipid motion in isotropic bicelles. *Langmuir 21*, 7702−7709.
(39) Cantor, C. R., and Schimmel, P. R. (1980) Size and shape of macromolecules, in *Biophysical Chemistry Part II: Techniques for the Study of Biological Structure and Function*, W.H. Freeman, San Fransisco.
(40) Lind, J., Nordin, J., and Mäler, L. (2008) Lipid dynamics in fast-tumbling bicelles with varying bilayer thickness: Effect of model transmembrane peptides. *Biochim. Biophys. Acta 1778*, 2526−2534.
(41) Ye, W., Liebau, J., and Mäler, L. (2013) New membrane mimetics with galactolipids: Lipid properties in fast-tumbling bicelles. *J. Phys. Chem. B 117*, 1044−1050.
(42) Lindström, F., Williamson, P. T., and Gröbner, G. (2005) Molecular insight into the electrostatic membrane surface potential by 14N/31P MAS NMR spectroscopy: Nociceptin-lipid association. *J. Am. Chem. Soc. 127*, 6610−6616.
(43) Kowalewski, J., and Mäler, L. (2006) *Nuclear Spin Relaxation in Liquids: Theory, Experiments, and Applications*, Taylor & Francis Group, New York.
(44) Malouin, F., Chamberland, S., Brochu, N., and Parr, T. (1991) Influence of growth media on *Escherichia coli* cell composition and ceftazidime susceptibility. *Antimicrob. Agents Chemother. 35*, 477−483.
(45) Leduc, M., and Schaechter, M. (1978) Size of the lipid precursor pool in *Escherichia coli*. *J. Bacteriol. 133*, 1038.
(46) Bennett, B. D., Kimball, E. H., Gao, M., Osterhout, R., Van Dien, S. J., and Rabinowitz, J. D. (2009) Absolute metabolite concentrations and implied enzyme active site occupancy in *Escherichia coli*. *Nat. Chem. Biol. 5*, 593−599.
(47) Axe, D. D., and Bailey, J. E. (1995) Transport of lactate and acetate through the energized cytoplasmic membrane of *Escherichia coli*. *Biotechnol. Bioeng. 47*, 8−19.
(48) Rosenthal, A. Z., Kim, Y., and Gralla, J. D. (2008) Regulation of transcription by acetate in *Escherichia coli*: In vivo and in vitro comparisons. *Mol. Microbiol. 68*, 907−917.
(49) Arrondo, J. L. R., and Goni, F. M. (1998) Infrared studies of protein-induced perturbation of lipids in lipoproteins and membranes. *Chem. Phys. Lipids 96*, 53−68.
(50) Bechinger, B., Ruysschaert, J., and Goormaghtigh, E. (1999) Membrane helix orientation from linear dichroism of infrared attenuated total reflection spectra. *Biophys. J. 76*, 552−563.
(51) Szalontai, B., Nishiyama, Y., Gombos, Z., and Murata, N. (2000) Membrane dynamics as seen by fourier transform infrared spectroscopy in a cyanobacterium, *Synechocystis* PCC 6803: The effects of lipid unsaturation and the protein-to-lipid ratio. *Biochim. Biophys. Acta 1509*, 409−419.
(52) Blume, A. (1996) Properties of lipid vesicles: FT-IR spectroscopy and fluorescence probe studies. *Curr. Opin. Colloid Interface Sci. 1*, 64−77.
(53) Moore, D. J., Gioioso, S., Sills, R. H., and Mendelsohn, R. (1999) Some relationships between membrane phospholipid domains, conformational order, and cell shape in intact human erythrocytes. *Biochim. Biophys. Acta 1415*, 342−348.
(54) Sunder, S., Mendelsohn, R., and Bernstein, H. (1976) Raman studies of the CH and CD stretching regions in stearic acid and some specifically deuterated derivatives. *Chem. Phys. Lipids 17*, 456−465.
(55) Sunder, S., Cameron, D., Casal, H., Boulanger, Y., and Mantsch, H. (1981) Infrared and Raman spectra of specifically deuterated 1,2-dipalmitoyl-*sn*-glycero-3-phosphocholines. *Chem. Phys. Lipids 28*, 137−147.
(56) Cameron, D. G., Casal, H. L., Mantsch, H. H., Boulanger, Y., and Smith, I. (1981) The thermotropic behavior of dipalmitoyl phosphatidylcholine bilayers. A fourier transform infrared study of specifically labeled lipids. *Biophys. J. 35*, 1−16.
(57) Jones, R. N. (1962) The infrared absorption spectra of deuterated esters: III. Methyl laurate. *Can. J. Chem. 40*, 301−320.
(58) Rohwedder, W. K., Scholfield, C. R., Rakoff, H., Nowakowska, J., and Dutton, H. J. (1967) Infrared analysis of methyl stearates containing deuterium. *Anal. Chem. 39*, 820−823.

(59) Bury-Moné, S., Nomane, Y., Reymond, N., Barbet, R., Jacquet, E., Imbeaud, S., Jacq, A., and Bouloc, P. (2009) Global analysis of extracytoplasmic stress signaling in *Escherichia coli*. *PLoS Genet. 5*, e1000651.
(60) Mutalik, V. K., Nonaka, G., Ades, S. E., Rhodius, V. A., and Gross, C. A. (2009) Promoter strength properties of the complete sigma E regulon of *Escherichia coli* and *Salmonella enterica*. *J. Bacteriol. 191*, 7279−7287.
(61) Nunn, W. D., and Cronan, J. E., Jr. (1976) Regulation of membrane phospholipid synthesis by the relA gene: Dependence on ppGpp levels. *Biochemistry 15*, 2546−2550.
(62) Gitter, B., Richter, W., Riesenberg, D., and Meyer, H. W. (1995) The appearance of cytoplasmic membranes of *Escherichia coli* cells in freeze-fracture electron microscopy after stringent and relaxed response. *FEMS Microbiol. Lett. 128*, 185−188.
(63) Rodionov, D. G., and Ishiguro, E. E. (1996) Dependence of peptidoglycan metabolism on phospholipid synthesis during growth of *Escherichia coli*. *Microbiology 142*, 2871−2877.
(64) Hayden, J. D., and Ades, S. E. (2008) The extracytoplasmic stress factor, σE, is required to maintain cell envelope integrity in *Escherichia coli*. *PLoS One 3*, e1573.
(65) Monné, M., Nilsson, I., Johansson, M., Elmhed, N., and von Heijne, G. (1998) Positively and negatively charged residues have different effects on the position in the membrane of a model transmembrane helix. *J. Mol. Biol. 284*, 1177−1183.
(66) Makoto, K., Masataka, I., and Masateru, N. (1978) Function of phospholipids on the regulatory properties of solubilized and membrane-bound *sn*-glycerol-3-phosphate acyltransferase of *Escherichia coli*. *Biochim. Biophys. Acta 529*, 237−249.
(67) Raetz, C. (1978) Enzymology, genetics, and regulation of membrane phospholipid synthesis in *Escherichia coli*. *Microbiol. Rev. 42*, 614−659.
(68) Green, P. R., Merrill, A., and Bell, R. M. (1981) Membrane phospholipid synthesis in *Escherichia coli*. Purification, reconstitution, and characterization of sn-glycerol-3-phosphate acyltransferase. *J. Biol. Chem. 256*, 11151−11159.